# Supporting Information

## Henriquez *et al.* 10.1073/pnas.0806300105

### SI Materials and Methods

**Genotyping of Mutant Mice.** All mutant mice were maintained on a C57/BL6 background. *Dvl1* mutant mice were kindly provided by T. Wynshaw-Boris (San Diego, CA) (1). Genotypes were determined by three-primer PCR using tail DNA. The primers used were as follows: forward, 5′-TCTGCCCAATTCCACCT-GCTTCTT-3′; reverse, 5′-CGCCGCCGATCCCCTCTC-3′, and the Neo primer 5′-AGGCCTACCCGCTTCCATT-GCTCA-3′.

**Analysis of Embryonic Mouse Diaphragms.** Diaphragms were fixed in 2% PFA at 4 °C overnight, permeabilized in PBS solution containing 0.5% Triton X-100, blocked (500 mM NaCl, 0.01 M phosphate buffer, 3% BSA, 5% goat serum) overnight, and then incubated with either Alexa-488 conjugated $\alpha$-BTX (Molecular Probes) alone overnight, or with mouse anti-neurofilament (clone 2H3 from Developmental Studies Hybridoma Bank) and anti-$\beta$III tubulin (TUJ1; Covance) antibodies for 72 h, followed by anti-mouse Alexa-594 conjugated secondary antibody (Molecular Probes) overnight. Fluorescent images of the right hemidiaphragms flat mounted in Fluoromount G (Southern Biotech) were captured with a Leica confocal microscope. Stacks were acquired at 1.1-$\mu$m intervals through the diaphragm and maximal projections were aligned using Photoshop and AChR cluster distribution analyzed. Eleven bins of 98 $\mu$m width centered at the phrenic nerve entry point were analyzed from each hemidiaphragm.

**Analysis of the Expression Levels of Wnt3.** Conditioned media (CM) were prepared by transient transfection of QT6 cells expressing Wnt3-HA, Sfrp1-Myc, or control RFP. The level of Wnt3 produced by transfected QT6 cells, embedded in collagen gel for *in vivo* experiments or their CM used in cultured myotubes, was assessed by Western blots using anti-HA or Myc antibodies and developed using ECL reagent kit (Amersham).

**Immunofluorescence Microscopy and Analyses of AChR Clusters.** PFA-fixed chick wing sections at stage HH27/28 (Hamilton2) were blocked with 5% goat serum and 5% horse serum in PBS solution and incubated with primary antibodies overnight at 4 °C. Antibodies to anti-myosin heavy chain (A4.1025) (3), SNAP25, HA, or Myc were detected with Alexa-546-conjugated secondary antibodies (Molecular Probes) and/or Alexa-488-conjugated $\alpha$-BTX for 2 h at room temperature. Fluorescent images were acquired with a Zeiss Axiovert 200M inverted fluorescence microscope. Images of AChR clusters of corresponding regions of implanted and contralateral control wings were captured in a 12 picture stack at 1-$\mu$m intervals. Metamorph software was used to obtain stack and two-dimensional de-convoluted images, an average threshold defined to include clusters observed in every picture of the series, and the number of AChR clusters automatically quantified. AChR clusters were scored in dorsal and ventral muscles over four sections covering the region where the implanted cells were located (i.e., between 20 and 120 $\mu$m from implanted cells). For C2C12 experiments, clusters with an area larger than 4.5 $\mu m^2$ (large clusters) were automatically scored using Metamorph software. Micro-clusters defined by area less than 4.5 $\mu m^2$ were counted similarly. A threshold was determined by comparing the number of clusters scored automatically with those counted manually. Myotube surfaces were manually traced and their area was calculated using Metamorph. Data are expressed as the number of AChR clusters per square millimeter of total myotube area and correspond to the average ± SEM of three independent experiments performed in duplicate. Blind experiments gave similar results.

**Rac and Rho Activation Assays.** Assays were performed in C2C12 myotubes using GST-PBD (Pak1 Rac1/cdc42 binding domain, Upstate) or GST-RBD (Rhotekin Rho binding domain; Upstate) according to the manufacturer's instructions. Briefly, C2C12 myotubes were treated with Wnt-containing conditioned medium or 200 pM agrin for 15 min at 37 °C, and then lysed with 25 mM Hepes pH 7.5, 150 mM NaCl, 1% Igepal CA-630, 10% glycerol, 25 mM NaF, 10 mM $MgCl_2$, 1 mM EDTA, 1 mM $Na_2VO_3$, 10 $\mu$g/ml leupeptin, and 10 $\mu$g/ml aprotinin. Total protein (600–800 $\mu$g) was incubated with 15 $\mu$l of GST-PBD-bound beads for 1 h at 4 °C. Beads were washed three times in the same buffer, and PBD-bound Rac1 or RBD-bound RhoA were eluted by incubating the beads for 5 min at 95 °C in Laemmli buffer. Proteins were separated in 15% SDS/PAGE, and visualized with specific anti-Rac1 (Upstate), anti-RhoA, or anti-Cdc42 antibodies (Santa Cruz Biotechnology). Total protein lysates were run as loading control.

To assess the role of Rac1 in microcluster formation, differentiated myotubes were transfected with GFP control or with DN-Rac1 using Fugene 6 reagent (Roche). After 16 h, cells were incubated with Alexa-488-conjugated $\alpha$-BTX for 1 h at 37 °C to visualize AChR clusters. Cells were treated for 15 min, 30 min, or 1 h with Wnt3 and/or agrin in the presence Alexa-488-conjugated $\alpha$-BTX before fixation and immunostaining.


1. Lijam N, *et al.* (1997) Social interaction and sensorimotor gating abnormalities in mice lacking Dvl1. *Cell* 90:895–905.
2. Hamburger V, Hamilton HL (1951) A series of normal stages in the development of the chick embryo. *J Morphol* 88:49–92.
3. Dan-Goor, M, Silberstein L, Kessel M, Muhlrad A (1990) Localization of epitopes and functional effects of two novel monoclonal antibodies against skeletal muscle myosin. *J Muscle Res Cell Motil* 11:216–226.

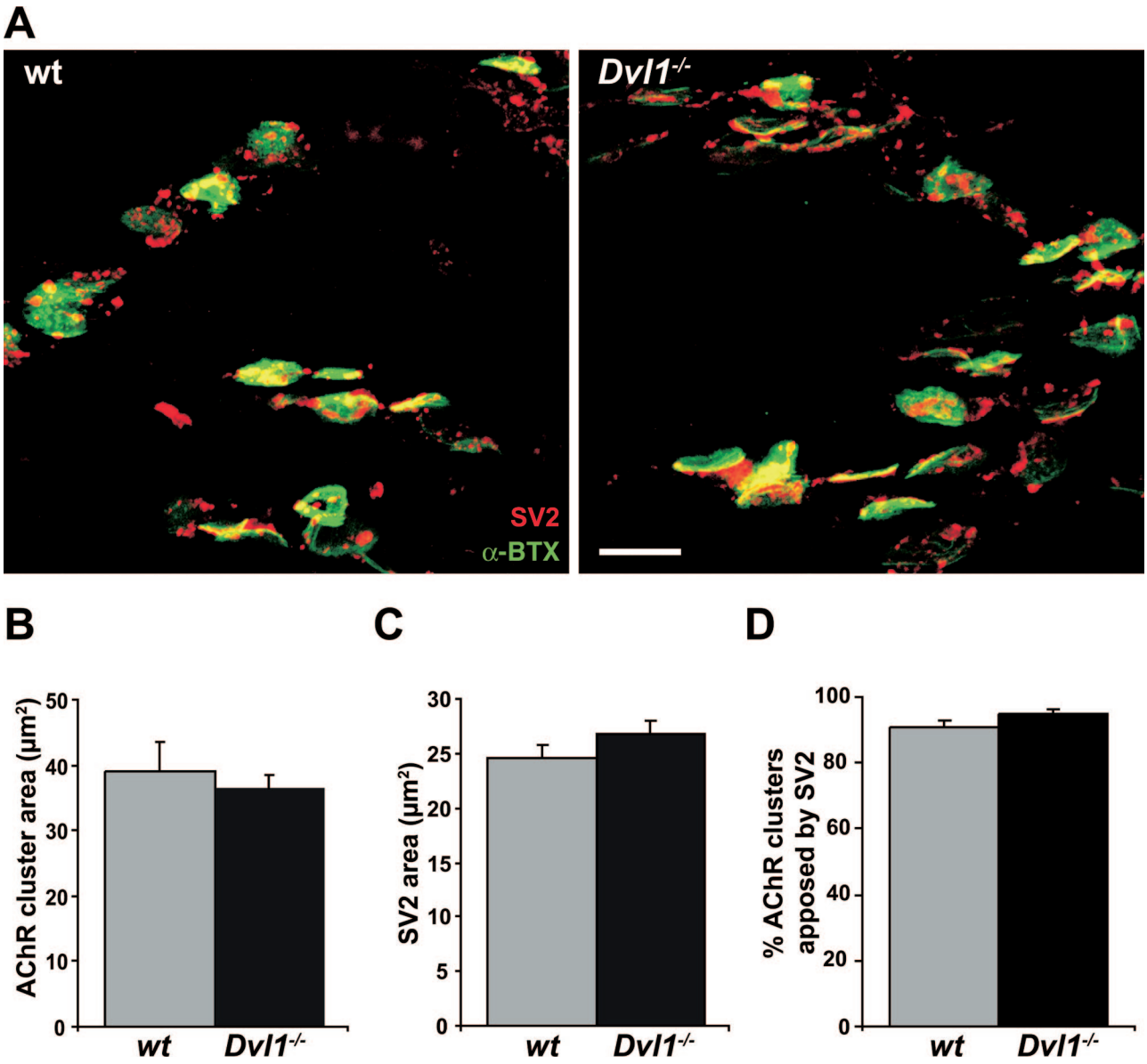


**Fig. S1.** *Dvl1* mutant diaphragm does not exhibit defects in the nerve terminal morphology. The size and apposition of AChR clusters and nerve terminals are similar in WT and *Dvl1*$^{-/-}$ diaphragms. (*A*) Representative maximal projections from E18.5 diaphragms stained with $\alpha$-BTX (green, labeling AChR clusters) and an anti-SV2 antibody (red, labeling nerve terminals). Analysis did not reveal any difference in the size of AChR clusters (*B*) or accumulation of the presynaptic marker SV2 (*C*). Furthermore, no difference in apposition of AChR clusters and presynaptic terminals was observed (*D*). Nine fields of view are shown from three diaphragms per genotype (Scale bar, 15 $\mu$m).

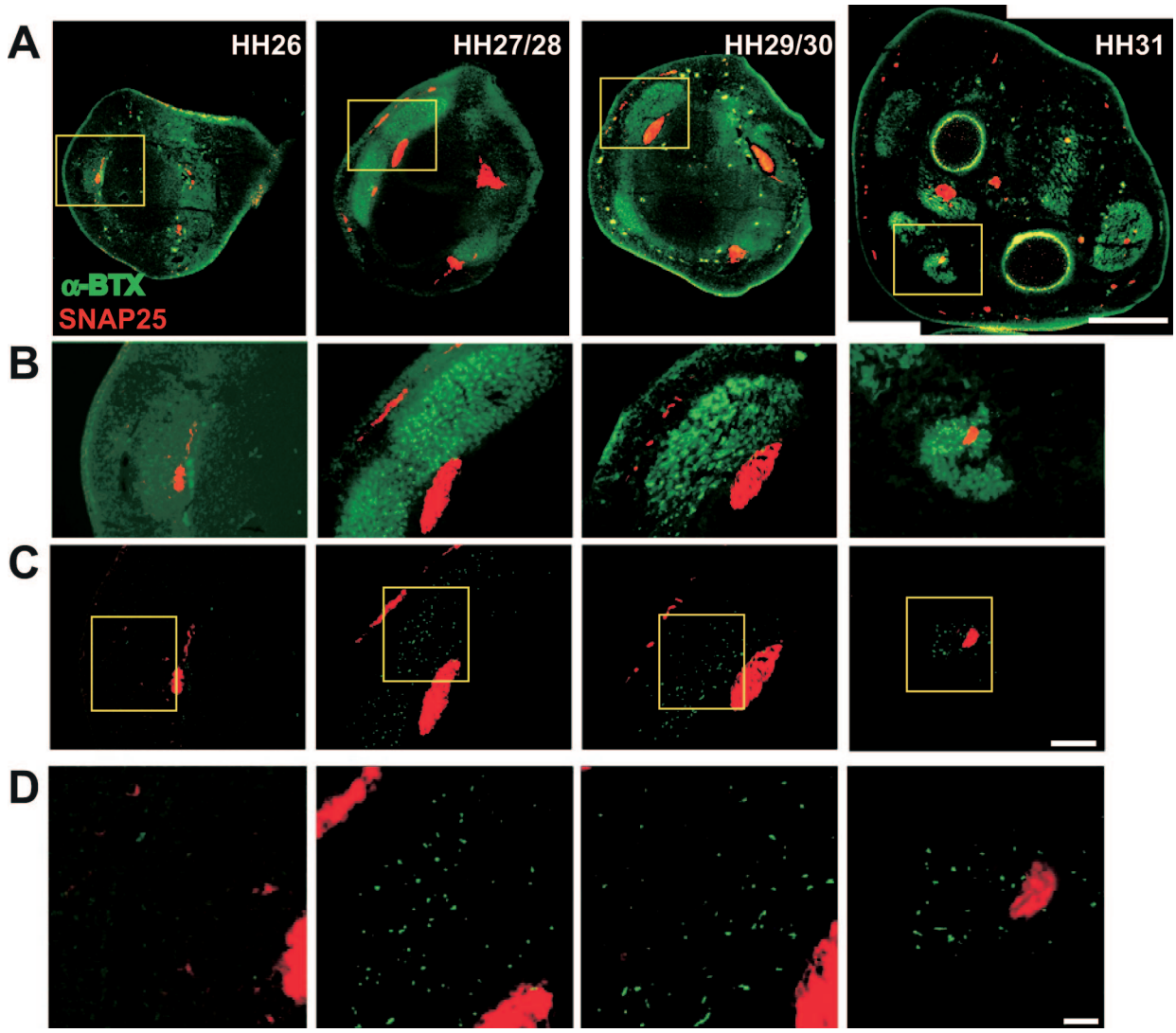


**Fig. S2.** AChR clustering profile during chick wing development. Embryonic chick wings at different stages were cryo-sectioned and stained to visualize nerve profiles (red) and AChR (green). (*A*) At low magnification, low-level widespread AChR becomes abundant on HH27/28 muscle, but declines as muscle matures. (*B*) A 12-picture stack shows widespread distribution of tiny AChR clusters and the appearance of larger clusters as fibers grow and mature. Compare the early-maturing region near the major nerve trunk in HH27/28 and HH28/29 (*C* and *D*). Deconvolution filtering reveals strong AChR clustering. Few AChR clusters were observed on the surface of HH26 muscle fibers. From HH27/28 onward, bigger and brighter AChR aggregates are evident on muscle regions near approaching nerve trunks. Squares in *A* and *C* are shown magnified in *B* and *D*, respectively. Dorsal muscle mass is to the left (Scale bars, 500 $\mu$m in *A*, 100 $\mu$m in *B* and *C*, and 25 $\mu$m in *D*).

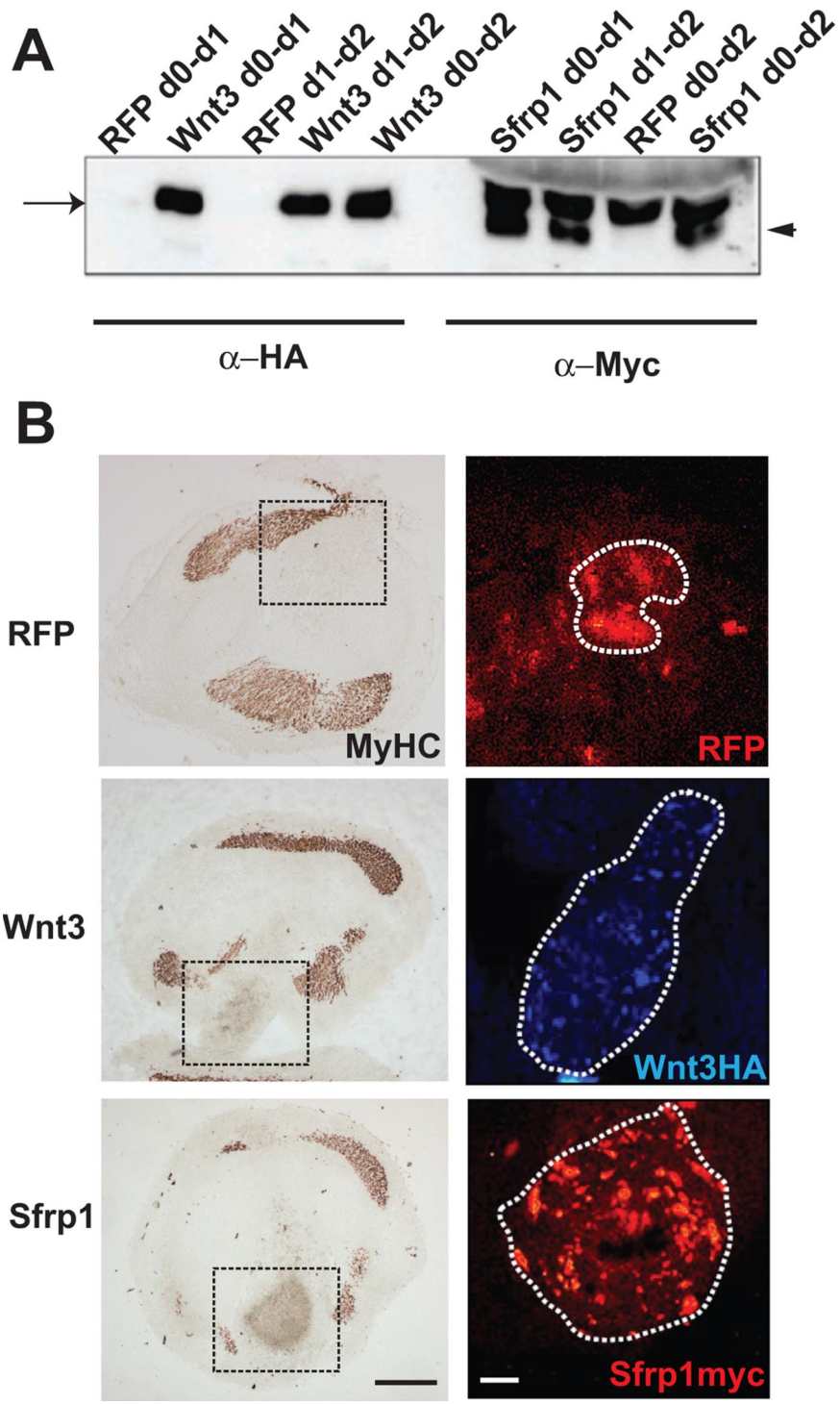


**Fig. S3.** Analyses of Wnt3 and Sfrp1 proteins in transplantation experiments. (*A*) The levels of Wnt3 and Sfrp1 proteins secreted by QT6 cells expressing RFP, Wnt3, or Sfrp1 were analyzed. The cells were embedded in collagen gels and incubated *in vitro* for 48 h. CM were collected during the first (d0–d1), the second (d1–d2), and over the 2-day (d0–d2) period of incubation and analyzed by Western blot using anti-HA (for Wnt3, *Left*) or anti-myc (for Sfrp1, *Right*) antibodies. Wnt3 (arrow) and Sfrp1 (arrowhead) proteins are constantly secreted from collagen gel-embedded QT6 cells over the 48 h of the *in vivo* experiment. (*B*) The expression of RFP control, Wnt3-HA, and Sfrp1-myc in implanted cells were analyzed in the limb at HH27/28. Immunodetection reveals that proteins are expressed within the implant in proximity to the muscle masses (stained for myosin heavy chain, *Left*) in the limb. (Scale bar: 500 $\mu$m *Left*, 100 $\mu$m.)

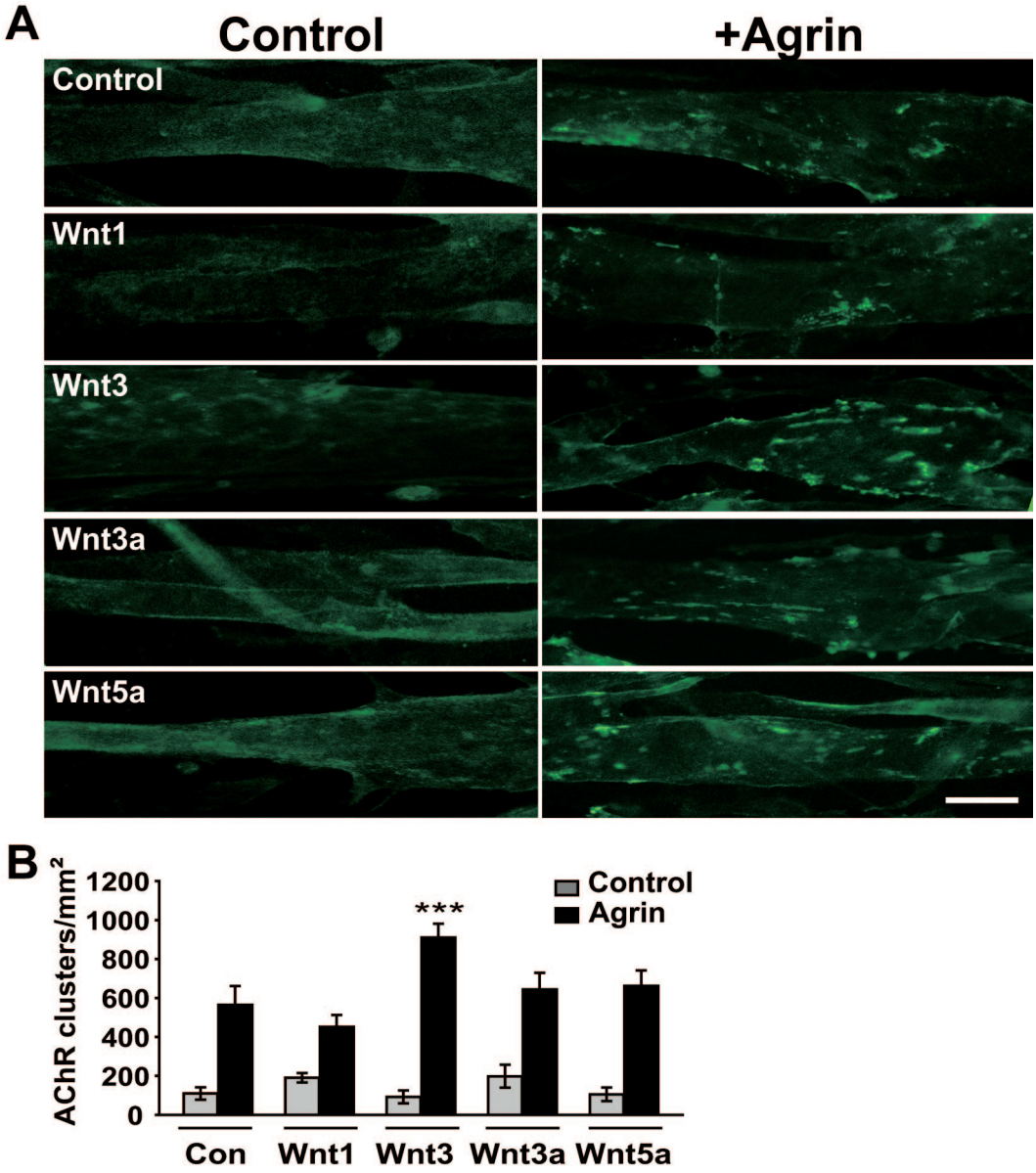


**Fig. S4.** Effect of different Wnts on agrin-induced AChR clustering. (*A*) Myotubes were treated with CM obtained from transient transfection of QT6 cells (expressing Wnt1-HA or Wnt3-HA), or with recombinant Wnt3a or Wnt5a in the presence or absence of agrin. (*B*) Wnt1, Wnt3a, or Wnt5a do not have a statistically significant effect on the ability of agrin to induce AChR clustering. (Scale bar, 40 $\mu$m.)

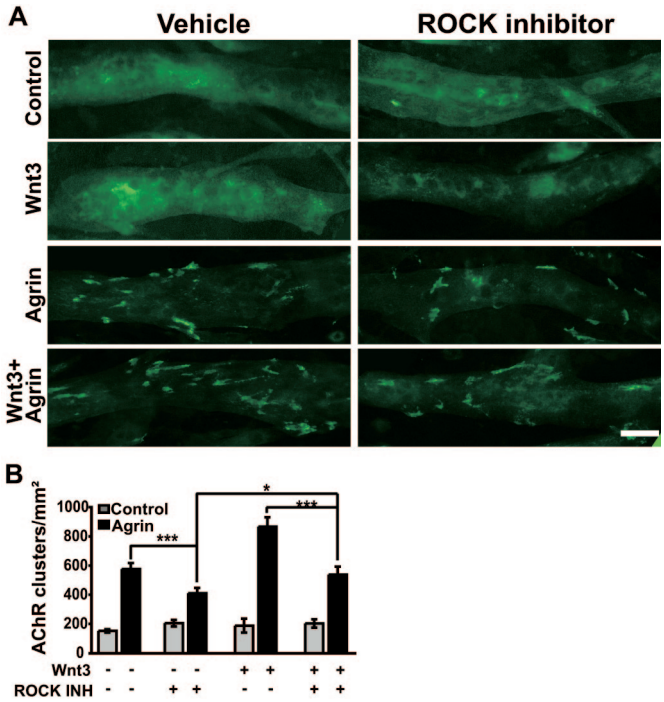


**Fig. S5.** ROCK signaling does not modify Wnt3 activity on cultured myotubes. Myotubes were incubated for 15 min with control or Wnt3 in the presence or absence of agrin. (*A*) Inhibition of ROCK by Y27632 reduces the number of AChR clusters induced by agrin as well as those formed in the presence of both agrin and Wnt3. (*B*) Quantification reveals that inhibition of ROCK significantly reduces AChR clustering in the presence of agrin (29%; ***, $P < 0.001$) or both Agrin and Wnt3 (38%; ***, $P < 0.001$). (Scale bar, 20 $\mu$m.)